

<http://www.glaciology.ethz.ch>

## ICEQUAKES AS PRECURSORS OF ICE AVALANCHES

J. FAILLETTAZ, M. FUNK, AND D. SORNETTE

**ABSTRACT.** A hanging glacier at the east face of Weisshorn broke off in 2005. We were able to monitor and measure surface motion and icequake activity for 21 days up to three days prior to the break-off. Results are presented from the analysis of seismic waves generated by the glacier during the rupture maturation process. Three types of precursory signals of the imminent catastrophic rupture were identified: (i) an increasing seismic activity within the glacier, (ii) a change in the size-frequency distribution of icequake energy, and (iii) a log-periodic oscillating behavior superimposed on power law acceleration of the inverse of waiting time between two icequakes. The analysis of the seismic activity gave indications of the rupture process and led to the identification of two regimes: a stable one where events are isolated and non correlated which is characteristic of diffuse damage, and an unstable and dangerous one in which events become synchronized and large icequakes are triggered.

### 1. INTRODUCTION

The fracturing of brittle heterogeneous material has often been studied at the lab scale using acoustic emission measurements (Johansen and Sornette, 2000; Nechad et al., 2005). These studies reported an acceleration of brittle damage before failure. Acoustic emission tools have already been used at meso-scale to find precursors to natural gravity-driven instabilities such as cliff collapse (Amitrano et al., 2005) or slope instabilities (Dixon and Spriggs, 2007; Kolesnikov et al., 2003). The present paper focuses on the acoustic emissions generated by an unstable glacier. To our knowledge, this is the first attempt to use these acoustic emissions to predict the catastrophic collapse of a glacier.

Ice mass break-off is a natural gravity-driven instability as found in the case of a landslide, rockfalls or mountain collapse. Rupture takes place within ice and propagates until the glacier collapses. This represents a considerable risk to mountain communities situated below, especially in winter, as an ice avalanche may drag snow in its train. An accurate prediction of this natural phenomenon must be made in order to prevent such dangerous occurrences. The first attempt to predict such icefalls was conducted in 1973 by Flotron (1977) and Röthlisberger (1981) on the Weisshorn hanging glacier. These authors measured the surface velocity of the unstable glacier and proposed an empirical function to fit the increasing surface velocities before break-off. This function describes an acceleration of the surface displacement following a power law up to infinity at a finite time  $t_c$ . Obviously, the real collapse will necessarily occur before  $t_c$ , but this method gives a good description of the surface velocity evolution until rupture. Recently, following Lüthi (2003) and Pralong et al. (2005), Faillettaz et al. (2008) showed evidence of an oscillatory behaviour superimposed on the general acceleration which enables a more accurate determination of the time of rupture. Faillettaz et al. (2008) showed also

---

*Key words and phrases.* glacier, rupture, prediction, icequakes.

an increase in icequake activity before the break-off. The aim of this paper is to present (i) a careful analysis of these seismic measurements, (ii) our conclusions in terms of rupture processes, and (iii) perspectives for forecasting.

Several studies have shown that glaciers can generate seismic signals called icequakes. Icequakes in Alpine glacier have been investigated in various contexts. Several types of source mechanisms have been postulated or assumed such as surface crevasse formation (e.g. Neave and Savage, 1970; Deichmann et al., 2000), stick-slip motion (Weaver and Malone, 1979; Roux et al., 2008), bottom crevasse formation due to increased basal drag during low subglacial water pressures (Walter et al., 2008) or resonant water-filled cavities (Metaxian et al., 2003).

In this study, the focus is on seismic activity generated by a cold hanging glacier before its collapse. The crucial features of this type of glacier are: (i) there is no sliding at the bedrock and (ii) there is no water within the ice. Precursory seismic signals were detected, and a change in the behavior occurred two weeks before the global rupture.

## 2. THE WEISSHORN GLACIER

The northeast face of the Weisshorn (Valais, Switzerland) is covered with unbalanced cold ramp glaciers (i.e., the snow accumulation is, for the most part, compensated by break-off, Pralong and Funk, 2006) located between 4500 m and 3800 m a.s.l., on a steep slope of 45 to 50 degrees. In winter, snow avalanches triggered by icefalls pose a recurrent threat to the village of Randa located some 2500 m below the glacier, and to transit routes to Zermatt (see Fig. 1). The Weisshorn hanging glacier broke off five times in the last 35 years (1973, 1980, 1986, 1999 and 2005); two of these events (in 1973 and 2005) were monitored in detail (Flotron, 1977; Faillettaz et al., 2008).

The total volume of the unstable ice mass was estimated at  $0.5 \times 10^6 \text{ m}^3$  by means of photogrammetry (Faillettaz et al., 2008). Because of the dangerous situation for the village of Randa, a monitoring system was installed to alert the population of an impending icefall.

An automatic camera (installed in September 2003 on the Bishorn, see Fig. 1) provided a detailed movie of the destabilization of the glacier. A first break-off occurred on March 24, 2005 (after 26.5 days of monitoring). Its estimated volume amounted to  $100,000 \text{ m}^3$  (comparable to the 1973 break-off with  $160,000 \text{ m}^3$ ). On March 31, 2005 a second rupture occurred, during which the major part of the glacier fell (after 33.5 days of monitoring). The volume of this second ice avalanche was estimated at  $400,000 \text{ m}^3$ .

A geophone was also installed near the upper crevasse (see Fig. 1) in order to record icequake activity before the final rupture. This signal is assumed to describe the crack (or damage) evolution within the ice mass during the failure process.

## 3. MEASUREMENTS AND RESULTS

A single geophone (Lennartz LE-3Dlite MkII, 3 orthogonal sensors, with eigenfrequency of 1 Hz) was installed in firn 30 cm below the surface near the upper crevasse (Fig. 1). A Taurus portable seismograph (Nanometrics inc.) was used to record the seismic activity of the glacier prior to its rupture with a sampling rate of 100 Hz. Unfortunately, the recorder failed on March 21, before the first break-off

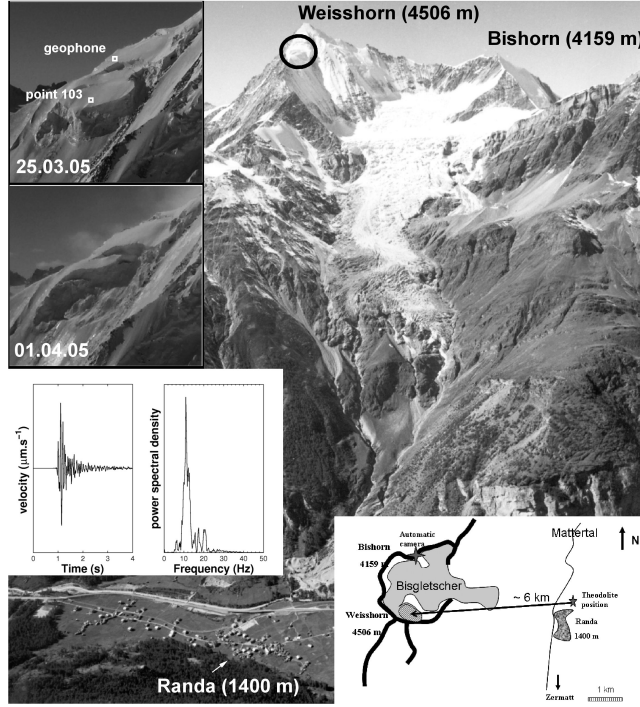


FIGURE 1. The east face of Weisshorn with the hanging glacier. The village of Randa and transit routes are visible in the valley. The ellipse indicates the location of the hanging glacier. The left insets show a closer frontal view of the hanging glacier on March, 25th 2005 before the second break-off (upper), and on April 1st, 2005 after the break-off (lower), including the positions of the geophone and stake 103 used for displacement measurements. Below these photographs, unfiltered velocity seismogram of a typical event (maximum amplitude  $2.5 \mu\text{m.s}^{-1}$ ) and its corresponding normalized power spectral density were drawn. The bottom right inset shows the general schematic view of the Weisshorn hanging glacier (dashed zone), and the monitoring setting (theodolite and automatic camera). Thick black lines indicate the mountain ridges, and the thin line represents the bottom of the valley.

event, because of battery problems. A first seismic analysis of these measurements was presented in Faillettaz et al. (2008).

**3.1. Signal characteristics.** The data show a high seismic emissivity from the hanging glacier during the time span of our observations. Roux et al. (2008) found two types of signal characteristics for icequakes. The first type is associated with small cracks and has a short and impulsive signal, associated with crevasse opening. Such icequakes lie in the 10-40 Hz band and therefore represent high-frequency events. The second type of event is associated with long and complex signals with high amplitude that can be linked with serac falls.

In the case of the Weisshorn hanging glacier, events with short and impulsive signals with similar spectra are observed (see Fig. 1), with dominant power contained in the 10-30 Hz frequency band. This observation is consistent with previous results (Roux et al., 2008; O’Neel et al., 2007)

This result is not surprising, as no serac falls could be observed during the time span of our observations (based on daily photographs). Since the sensor is very close to the sources, attenuation is low. The proximity of the source (less than 300 meters) gives rise to difficulties in distinguishing P and S waves. As the geophone is situated above the upper crevasse separating the active and the stable zone, compressive seismic waves (primary wave) are perturbed by the discontinuity of the material and therefore are less likely to be observed.

**3.2. Detection of events.** The detection of events was performed in the following way. First, we evaluated the root-mean-square (rms) of two concurrent time windows. The rms values over the previous 800 ms long-term average (LTA) window and the previous 80 ms short-term average (STA) windows were calculated and compared. When the ratio  $\gamma = \text{STA}/\text{LTA}$  exceeded a given threshold (equal here to 3), an event was detected and retained (Allen, 1978; Walter et al., 2008). We found a total of 1731 such icequakes during the 21 days preceding the break-off. Figure 2 shows the number of detected events per hour during the 21-day period of the ice chunk destabilization. An acceleration of the seismic activity was detected after 18 days of monitoring (i.e., one week before the first and two weeks before the main break-off).

**3.3. Size-frequency distribution of icequake energies.** In order to compare all icequakes and perform a size-frequency analysis, we first had to evaluate the size of each icequake. Seismic event sizes were estimated based on their signal energies as defined for a digitalized signal by (Evans [1979], in Amitrano et al. (2005))

$$(3.1) \quad E = \sum A^2 \delta t$$

where  $A$  is the signal amplitude and  $\delta t$  the sampling period. We made a manual selection of the beginning and the end of each signal and performed the discrete summation for the evaluated duration. This procedure allowed to determine the energy of every icequake.

The complementary cumulative size-frequency (also called “survival”) distribution (CSFD) of the icequake energy preceding the break-off was then determined. In order to study the temporal variation of the CSFD, we used a moving window of 100 events with a 10-event shift between successive windows. We analyzed the event size distribution corresponding to each window (Fig. 3 shows four typical windows).

Three different behaviors can be successively observed:

(i) For the windows located near the beginning of our measurements (up to  $t = 10$  d), the CSFD is well described by a power law distribution over at least 2 orders of magnitude, indicating a scale invariance of the acoustic emissions similar to that characterizing earthquakes. For earthquakes, the corresponding Gutenberg-Richter law is one of the most ubiquitous statistical regularity observed of earthquakes. It reads

$$(3.2) \quad N(> E) \sim E^{-\beta} ,$$

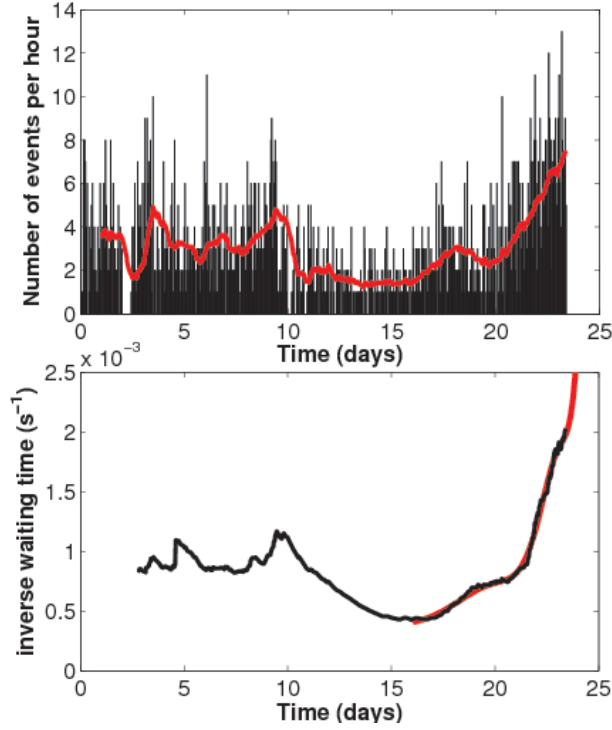


FIGURE 2. Top: Number of detected icequakes per hour (bars in black) as a function of time. In red is plotted the number of events per hour averaged on the last day of observation (sliding windows of 24 hours). Bottom: Inverse of waiting time ( $s^{-1}$ ) between two events as a function of time. Each point represents the mean of the inverse of waiting time between 2 events in a moving window containing 200 events, plotted as a function of the time of the last point of the window. In red is plotted the fit with the log-periodic law, indicating a critical time of 26.5 days. The glacier broke-off after 26 days.

where  $N(> E)$  is the number of events of energy greater than  $E$  and  $\beta$  is the Gutenberg-Richter exponent found empirically close to  $2/3$  for shallow earthquakes (depths  $< 70km$ ) in subduction and transform fault zones. Fig. 3 shows the evolution of the exponent  $\beta$  of the CSFD for icequakes. Up to  $t = 10$  d, the exponent  $\beta$  is found compatible with the earthquake value  $\beta = 0.65 \pm 0.1$ .

(ii) From  $t = 10$  d to  $t = 15$  d, the exponent  $\beta$  exhibits a rapid shift followed by a stabilization to a value  $\beta = 1.4 \pm 0.1$ , suggesting a change of behavior of the damage process developing in the ice mass. Pisarenko and Sornette (2003) have associated a change of the exponent  $\beta$  with a change in the rupture process: In their study, they confirmed previous observations that the exponent  $\beta$  of the Gutenberg-Richter law for shallow events is significantly smaller for subduction zones ( $\beta \simeq \frac{2}{3}$ ) compared to mid-ocean ridges ( $\beta \simeq \frac{4}{3}$ ). They proposed an explanation of these two exponent regimes based on two remarks. First, large exponents  $\beta$  are found in

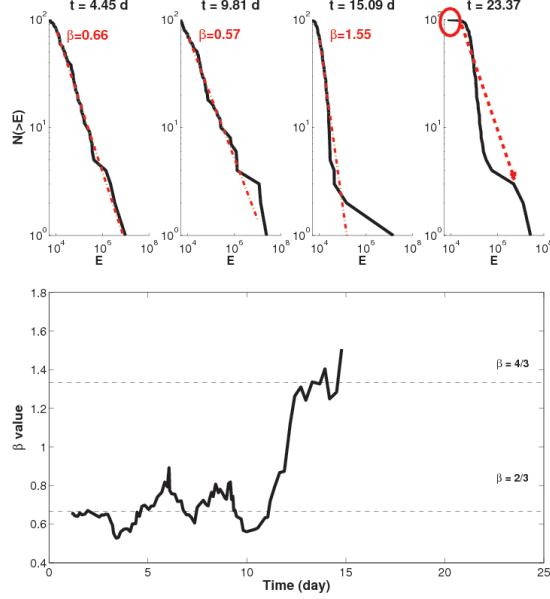


FIGURE 3. The four plots at the top show the complementary cumulative size-frequency distribution (CSFD) of icequake energies obtained in four windows of 100 events each, ending at the time indicated in the panels. The lower plot shows the evolution of the exponent  $\beta$  of the power law fitting the CSFD obtained in running windows of 100 events. The exponent  $\beta$  has been estimated with the Maximum Likelihood method. After day 15, the CSFD cannot anymore be fitted with a pure power law, because a significant “shoulder” appears in the tail.

the distribution of acoustic emission energies recorded for heterogeneous materials brought to rupture, for which damage is mainly in the form of weak shear zones and open cracks. In other words, large exponents  $\beta$  characterize mainly an open crack mode of damage. Second, when damage develops in the form of “dislocations” or mode II cracks, with slip mode of failure and with healing, the exponent  $\beta$  is found smaller than 1. This suggests that the low values of  $\beta \simeq 2/3$  obtained for our data in the first 10 days of recording are associated with a stable, slow and diffuse “dislocation-like” damage process. In the subsequent days, the increase of the exponent  $\beta$  up to  $1.4 \pm 0.1$  can be interpreted as revealing a transition to a mode of damage controlled more and more by crack openings.

(iii) For the time windows near the end of our observation period (after  $t = 15$  d), the CSFD of icequake energies no longer conforms to a power law (upper right panel of Fig. 3). The tail of the distribution develops a strong shoulder, indicating a change in the damage mechanism. The clear deficit of icequakes with small energies and the excess of large “characteristic” events is fully compatible with the evolution of the second regime dominated by crack-like events which, by their proliferation and fusion, progressively nucleate the run-away macro-crack responsible for the

final avalanche associated with a rather clean crack-like rupture, as shown in Fig. 1.

**3.4. Accelerating rate of icequakes.** The time evolution of the rate of icequakes is well-captured by that of the inverse of the mean time lag between two consecutive icequakes. Fig. 2 shows this inverse mean time lag in a moving window containing 100 events as a function of the time of the last point of the window. One can clearly observe a general acceleration of the icequake activity a few days before the collapse of the glacier. The beginning of this acceleration observed for  $t > 15$  d coincides approximately with the transition to the crack-dominated damage regime, that we have identified from the increase of the exponent  $\beta$  shown in Fig. 3.

In addition to its acceleration developing in the last few days preceding the collapse, the rate  $s(t)$  of icequakes is also characterized by accelerating oscillations, which are well-fitted by the log-periodic power law defined by the equation:

$$(3.3) \quad s(t) = s_0 + a(t_c - t)^m \left[ 1 + C \sin\left(2\pi \frac{\ln(t_c - t)}{\ln(\lambda)} + D\right) \right].$$

Here,  $s_0$  is a constant,  $t_c$  is the critical time at which the global collapse is expected,  $m < 1$  is the power law exponent quantifying the acceleration,  $a$  is a constant,  $C$  is the relative amplitude of the oscillations with respect to the overall power law acceleration,  $\lambda$  is the so-called “scaling ratio” associated with the log-periodicity of expression (3.3) and  $D$  is the phase of the log-periodic oscillation. The best fit of the rate of icequakes to expression (3.3) is shown in red in Fig. 2. It predicts a critical time  $t_c$  very close (half-a-day) to the time when the glacier broke-off, suggesting a novel method to predict future glacier failures by monitoring icequake rates in real time.

Such log-periodic power law has been found to be an efficient practical tool to model acoustic emission data (see Johansen and Sornette (2000) and references therein). The log-periodic oscillations in particular provide an important additional information to stabilize the fits and get better estimations of the critical time  $t_c$ . Log-periodic oscillations are the signature of a weaker kind of scale invariance called discrete scale invariance, appearing after the partial breaking of a continuous scale symmetry. In quasi-static growth models of ensembles of interacting cracks, discrete scale invariance has been shown to originate from the existence of a cascade of Mullins-Sekerka instabilities (Huang et al., 1997). This view is coherent with the results obtained in the previous section in which we have argued that, for  $t > 15$  d, crack growth and coalescence dominate, developing into a collective crack damage mode leading eventually to the global collapse. Furthermore, the log-periodic power law model was previously found to provide a good description of the surface motion of different points on this glacier (Faillottaz et al., 2008), showing the convergent evidence offered by these two metrics (icequake rate and surface deformation).

#### 4. SUMMARY AND PROSPECTIVE

We have presented and studied a unique dataset of icequakes recorded in the immediate vicinity of the hanging Weisshorn glacier over 21 days prior to its rupture. While measurement records ceased unfortunately 3 days before the first break-off and 10 days before the larger subsequent one, we have nevertheless been able to obtain a coherent quantitative picture of the damage process developing before the impending glacier collapse. Our main results include the demonstration of (i) a

clear increase of the icequake activity within the glacier (measured as the inverse of the waiting time between successive icequakes) starting approximately 7 days before the first avalanche, (ii) a two-step evolution of the size-frequency distribution of icequake energies, characterizing a first transition to a crack-like dominated damage followed by a second transition in which large characteristic cracks are thought to prepare the nucleation of the run-away rupture, and (iii) a log-periodic oscillatory behavior superimposed on a power law acceleration of the rate of icequakes, which is a typical of the hierarchical cascade of rupture instabilities found in earlier reports on the acoustic emissions associated with the failure of heterogeneous materials.

Provided that technical solutions are found to ensure continuous icequake recordings in the difficult high-altitude mountain conditions, our results open the road for real-time diagnostics of impending glacier failure. The next steps towards this goal include (a) developing an automatic seismic data processing in real time (which include the automatic detection of icequakes and the determination of their energy), (b) processing these data with the statistical tools developed here and (c) performing systematic reliability tests to access the rate of false alarms (false positives or errors of type I) versus missed events (false negatives or errors of type II). Step (c) is necessary for an informed cost-benefit analysis of the societal and economic impacts of the proposed real-time forecast methodology.

**Acknowledgements:** The Institute of Geophysics at the ETHZ is gratefully acknowledged for allowing us the use of their instruments. Thanks are extended to Fabian Walter for fruitful discussions.

## REFERENCES

- Allen, R. V., 1978. Automatic earthquake recognition and timing from single traces. *Bull. Seismol. Soc. Am.*, **68**, (5), 1521-1532.
- Amitrano, D., Grasso J.-R. and Senfaute, G., 2005. Seismic precursory patterns before a cliff collapse and critical point phenomena, *Geophys. Res. Lett.*, **32**:L08314.
- Deichmann, N., Ansorge, J., Scherbaum, F., Aschwanden, A., Bernhardt, F. and Gudmundsson, G. H., 2000. Evidence for deep icequakes in an Alpine glacier, *Ann. Glaciol.*, **31**, 85-90.
- Dixon, N. and Spriggs, M., 2007. Quantification of slope displacement rates using acoustic emission monitoring, *Can. Geotech. J.*, **44**, 966-976.
- Faillettaz, J., Pralong, A., Funk, M. and Deichmann, N., 2008. Evidence of log-periodic oscillations and increasing icequake activity during the breaking-off of large ice masses. *J. Glaciol.*, **57**, (187), 725.
- Flotron, A., 1977. Movement studies on hanging glaciers in relation with an ice avalanche, *J. Glaciol.*, **19** (81), 671-672.
- Huang, Y., Ouillon, G., Saleur H. and Sornette, D., 1997. Spontaneous generation of discrete scale invariance in growth models, *Phys. Rev. E*, **55** (6), 6433-6447.
- Johansen, A. and Sornette, D., 2000. Critical ruptures. *Eur. Phys. J. B*, **18**, 163.
- Kolesnikov, Yu. I., Nemirovich-Danchenko, M. M., Goldin, S. V. and Seleznev V. S., 2003. Slope stability monitoring from microseismic field using polarization methodology. *Nat. Haz. Earth Sys. Sc.*, **3**, 515-521.
- Lüthi, M., 2003. Instability in glacial systems, Milestones in Physical Glaciology: From the Pioneers to a Modern Science, 180, 63-70, VAW, ETH-Zürich.
- Métaxian, J.P., Araujo, S., Mora, M. and Lesage, P., 2003. Seismicity related to the glacier of Cotopaxi Volcano, Ecuador, *Geophys. Res. Lett.*, **30** (9), 1483.



- Neave, K. G. and Savage, J. C., 1970. Icequakes at Athabasca Glacier. *J. Glaciol.*, **49**, 587-598.
- Nechad, H., Helmstetter, A., El Guerjouma, R. and Sornette, D., 2005. Andrade and Critical Time-to-Failure Laws in Fiber-Matrix Composites: Experiments and Model, *J. Mech. Phys. Solids*, **53**, 1099-1127.
- O’Neel, S., Marshall, H. P., McNamara, D.E. and Pfeffer, W. T., 2007. Seismic detection and analysis of icequakes at Columbia Glacier, Alaska. *J. Geophys. Res.*, **112**, F03S23.
- Pisarenko, V.F. and Sornette, D., 2003. Characterization of the frequency of extreme earthquake events by generalized Pareto distribution, *Pure Appl. Geophys.*, **160**, 2343-2364.
- Pralong, A. and M. Funk, M., 2006. On the instability of avalanching glaciers, *J. Glaciol.*, **52** (176), 31-48.
- Pralong, A., Birrer, C., Stahel, W. and Funk, M., 2005. On the Predictability of Ice Avalanches, *Nonlin. Processes Geophys.*, **12**, 849-861.
- Röthlisberger, H., 1981. Eislawinen und Ausbrüche von Gletscherseen, in P. Kasser (Ed.), *Gletscher und Klima - glaciers et climat*, Jahrbuch der Schweizerischen Naturforschenden Gesellschaft, wissenschaftlicher Teil 1978, pp 170-212, Birkhäuser Verlag Basel, Boston, Stuttgart.
- Roux, P.-F., Marsan, D., Metaxian, J.-P., O’Brien, G. and Moreau L., 2008. Microseismic activity within a serac zone in an alpine glacier (Glacier d’Argentière, Mont-Blanc, France). *J. Glaciol.*, **54**, (184), 157.
- Walter, F., Deichmann, N. and Funk, M., 2008. Basal icequakes during changing subglacial water pressures beneath Gornergletscher, Switzerland. *J. Glaciol.*, **54**, (186), 511.
- Weaver, C. and Malone, S., 1979. Seismic evidence for discrete glacier motion at the rock-ice interface. *J. Glaciol.*, **23**, (89), 171.

VAW, ETH ZÜRICH, LABORATORY OF HYDRAULICS, HYDROLOGY AND GLACIOLOGY, SWITZERLAND

*E-mail address:* faillettaz@vaw.baug.ethz.ch

VAW, ETH ZÜRICH, LABORATORY OF HYDRAULICS, HYDROLOGY AND GLACIOLOGY, SWITZERLAND

*E-mail address:* funk@vaw.baug.ethz.ch

DEPARTMENT OF MANAGEMENT, TECHNOLOGY AND ECONOMICS, ETH ZÜRICH

DEPARTMENT OF EARTH SCIENCES, ETH ZÜRICH

INSTITUTE OF GEOPHYSICS AND PLANETARY PHYSICS, UCLA

*Current address:* Department of Management, Technology and Economics, ETH Zürich, Switzerland

*E-mail address:* dsornette@ethz.ch